

## SPECTROSCOPIC ELLIPSOMETRY ANALYSIS OF ANTIMONY TRISULFIDE ( $\text{Sb}_2\text{S}_3$ ) THIN FILM

N. DRISSI<sup>a,b</sup>, W. NOUIRA<sup>d,\*</sup>, M. GASSOUMI<sup>c,d</sup>

<sup>a</sup>*Department of Physics, Faculty of Science, King Khalid University, P. O. Box 9004, Abha, 61413, Saudi Arabia*

<sup>b</sup>*Laboratory of Materials, Organization and Properties (LMOP), Campus Universities, El Manar, 2092 Tunis, Tunisia*

<sup>c</sup>*Department of Physics, College of Sciences, Qassim University, 51452, Buryadh, Saudi Arabia*

<sup>d</sup>*Research Unit Advanced Materials and Nanotechnologies, ISSAT of Kasserine, university of Kairouan, BP 471, Kasserine 1200, Tunisia*

In the present research paper, thin films of antimony trisulfide ( $\text{Sb}_2\text{S}_3$ ) were successfully deposited on glass substrates. The effect of thickness on the structural and optical properties of antimony trisulfide ( $\text{Sb}_2\text{S}_3$ ) thin films is studied. The optical constants ( $n$ ,  $k$ ) and film thicknesses of  $\text{Sb}_2\text{S}_3$  thin films were obtained by fitting the ellipsometric parameters ( $\psi$  and  $\Delta$ ) data using three-layer model systems in the wavelength range of 400–1800 nm. It is found that the refractive index  $n$  increases with an increase of the film thickness. The structural investigations are performed by Scanning electron microscopy SEM (the Grain size increased with the film thickness). We demonstrate generalized ellipsometry for precise measurement of the principal indices of refraction and the extinction coefficients.

(Received May 2, 2020; Accepted September 11, 2020)

*Keywords:*  $\text{Sb}_2\text{S}_3$  thin film, Spectroscopic ellipsometry, SEM, Refractive index

### 1. Introduction

Antimony trisulphide thin films ( $\text{Sb}_2\text{S}_3$ ) is a V–VI semiconductor compound, and has gained considerable attention recently in the fabrication of various optoelectronics, photonic devices, and in the nanotechnology industry. Also  $\text{Sb}_2\text{S}_3$  have gained much attention during the past two decades due to their special properties such as high refractive index [1], well defined quantum size effects [2], photosensitive and thermo electric properties [3]. Many researchers earlier to its applications in microwave devices [4–7] ascribe the technological importance of  $\text{Sb}_2\text{S}_3$ . Among the available chalcogenides, pure and doped  $\text{Sb}_2\text{S}_3$  thin films are used in solar energy conversion, thermoelectric cooling technologies and as photoconductive target for Videocon type of television camera [6, 7]. Amorphous and crystalline thin films of antimony trisulphide were prepared many workers have obtained  $\text{Sb}_2\text{S}_3$  thin films by various technique as the chemical bath deposition [8, 9], the sol-gel method [10], vacuum evaporation method [6, 11] and have studied the effect of deposition conditions on the physical properties of the thin films. Among these methods used for the preparation of  $\text{Sb}_2\text{S}_3$  thin films, the chemical bath deposition method is often preferred because, it offers large possibilities to modify the deposition conditions so as to obtain films with required structure and physical properties for specific applications [7–12].

Spectroscopic ellipsometry (SE) is a non-destructive and sensitive technique for measuring the optical response of materials. By measuring the change in the polarization state, i.e. psi ( $\psi$ ) and delta ( $\Delta$ ), of the light reflected off the surface of a film and then utilizing an appropriate optical/dispersion model, one can extract precisely the optical properties and determine accurately the thickness of the film under study. In this paper, we report on the

\* Corresponding authors : [widednouira@yahoo.fr](mailto:widednouira@yahoo.fr)

preparation of structure films with different thicknesses of  $\text{Sb}_2\text{S}_3$ . The optical properties of films with different thicknesses of  $\text{Sb}_2\text{S}_3$  are investigated in terms of SE by using three-layer models.

## 2. Experimental details

The  $\text{Sb}_2\text{S}_3$  thin films with various thicknesses in the range 300-800 nm were deposited on un-heated glass substrates by thermal vacuum evaporation. The pressure during the evaporation was maintained at  $10^{-5}$  Torr. A chromel–alumel thermocouple monitored the substrate temperature. The deposition temperature of the films was  $50^\circ\text{C}$ , with heating only due to radiation from the crucible.

### 2.1. Characterization of the films

The SE parameters ( $\psi$  and  $\Delta$ ) for  $\text{Sb}_2\text{S}_3$  films were measured with a rotating-compensator instrument (J.A. Woollam Corporation, M-2000) in the wavelength range of 400–1800 nm. The data were acquired with angles of incidence varying from  $55^\circ$  to  $75^\circ$ . All the measurements were made at room temperature. The optical constants of the  $\text{Sb}_2\text{S}_3$  films were determined by fitting the model function to the measured data using J.A. Woollam Corporation-developed WVASE32 program. The surface structure was studied Scanning electron microscopy (SEM), techniques are employed to analyze the surface morphology of the films deposited.

## 3. Results and discussion

### 3.1. Scanning electron microscopic studies (SEM)

The surface morphology of the  $\text{Sb}_2\text{S}_3$  thin films has been studied by scanning electron microscopy. Fig.1. reveals the SEM micrographs of the  $\text{Sb}_2\text{S}_3$  thin films for different thickness (300, 500 & 800nm). He reveals several small grains are found to agglomerate and form a few larger grains (Fig. 1).

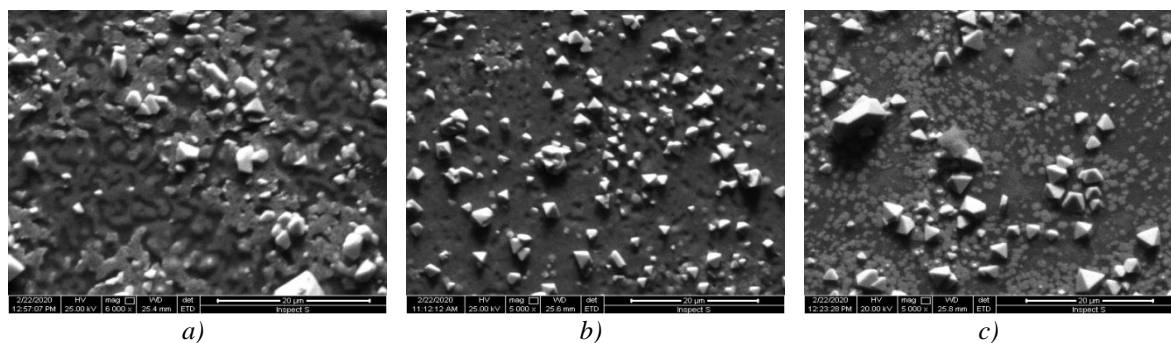


Fig. 1. Top view SEM images of the  $\text{Sb}_2\text{S}_3$  thin films for different thickness, a)300 nm; b)500nm; c)800 nm

The grains are found to be larger due to fusion of small crystallites. The overgrowth of particles is clearly seen from the SEM micrographs with increase in thickness of  $\text{Sb}_2\text{S}_3$  thin films. From the SEM studies the nature of the spherical grains are confirmed. The average grains size to be increased significantly due to the thickness.

### 3.2. Calculation of optical constants in terms of optical spectroscopic ellipsometry

The optical properties of  $\text{Sb}_2\text{S}_3$  thin films were primarily studied by SE, which measures the relative changes in amplitude and phase of the linearly polarized monochromatic incident light upon oblique reflection from the film surface. Appropriate experimental setups are required that can determine non-redundant optical parameters from a general anisotropic sample. Generalized ellipsometry (GE) comprises theory and experiment of anisotropy in layered samples. The

experimental parameters obtained by standard SE ( $\psi$  and  $\Delta$ ) are related to the microstructure and optical properties as defined by the following equation [19]:

$$\rho = \frac{r_p}{r_s} = \tan \psi \exp(i\Delta) \quad (1)$$

Here  $r_s$  and  $r_p$  are the complex Fresnel's reflection coefficients of the light polarized parallel ( $r_p$ ) and perpendicular ( $r_s$ ) to the plane of incidence, respectively. The layer model analysis, based on Fresnel's coefficients of reflection, was performed on the measured ellipsometric angles. The spectral dependences of  $\psi$  and  $\Delta$  were fitted in an appropriate model to extract the film thickness and optical constants, i.e. the refractive index ( $n$ ) and the extinction coefficient ( $k$ ), using a least-square regression analysis and a weighted root-mean-square error function. The ellipsometric study, by a three-layer model: upper layer (rough layer)/absorbing  $\text{Sb}_2\text{S}_3$  layer/glass substrate. The upper layer corresponds to the microscopic roughness obtained by SE is well correlated with the mean square error (MSE). The program is based on least-square regression to obtain the unknown fitting parameters and their maximum confidence limit. The procedure is to vary the fitting parameters to minimize the difference between the measured and calculated  $\psi$  and  $\Delta$  values. The Levenberg–Marquardt regression

Algorithm was used for minimizing the MSE [20]:

$$MSE = \frac{1}{2N-M} \sum_{i=1}^N \left( \left( \frac{\psi_i^{mod} - \psi_i^{exp}}{\sigma_{\psi,i}^{exp}} \right)^2 + \left( \frac{\Delta_i^{mod} - \Delta_i^{exp}}{\sigma_{\Delta,i}^{exp}} \right)^2 \right) \quad (2)$$

which has been used to judge the quality of the fit between the measured and the modeled data and is minimized in the fit. Here  $N$  is the number of measured  $\psi$  and  $\Delta$  pairs included in the fit,  $M$  is the number of fit parameters and  $i$  is the summation index.

Also,  $\psi_i^{exp}$ ,  $\Delta_i^{exp}$  and  $\psi_i^{mod}$ , and  $\Delta_i^{mod}$  are the experimental and modeled values of  $\psi$  and  $\Delta$ , respectively.  $\sigma_{\psi,i}^{exp}$  and  $\sigma_{\Delta,i}^{exp}$  are the experimental standard deviations in  $\psi$  and  $\Delta$ , respectively, which are calculated from the know error bars on the calibration parameters and the fluctuation of the measured data over the averaged cycle of the rotating polarizer and analyzer. Equation (2) has the  $2N$  and  $M$  in the prefatory because there are two measured values included in the calculation for each  $\psi$  and  $\Delta$  pair. The calculated data the  $\psi_i^{th}$  and  $\Delta_i^{th}$  are generated by using appropriate models as shown in figures 2(a-b-c) with corresponding dispersion relations [21]. The spectral dependences of  $\psi$  and  $\Delta$  determined for  $\text{Sb}_2\text{S}_3$  films on glass substrate are depicted in figures 3(a-b-c), respectively; the spectra show Fabray–Perot interference oscillations over the entire wavelength range originating from multiple reflections within the films [22].

Figs. 2(a-b-c) shows good agreement between the measured data (symbols) and the model fit (line) in the entire wavelength range measured.

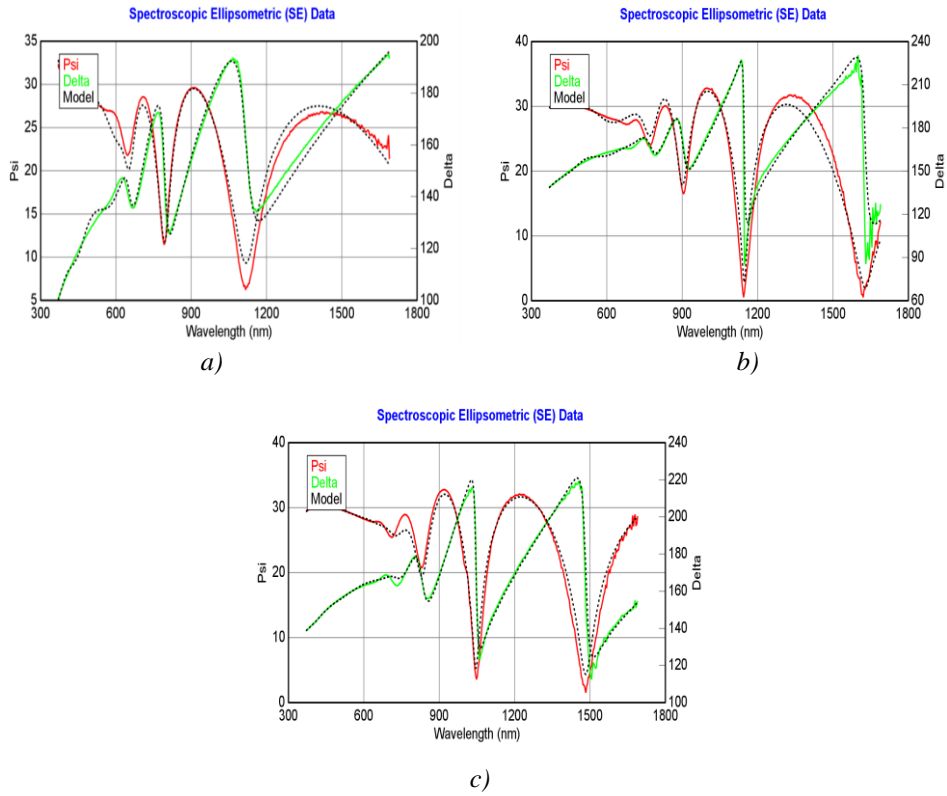


Fig. 2. a-b-c:  $\Psi$  and  $\Delta$  spectra obtained from spectroscopic ellipsometry for  $Sb_2S_3$  thin film at an angle of incidence of  $60^\circ$ . The continuous lines represent the model fit.

We note that the shapes of the curves with their particular interference peaks are correctly reproduced but slight differences between experimental and calculated parameters could be observed. The estimated thicknesses for the surface roughness layer and for the  $Sb_2S_3$  dense layer are shown in the insets of Figs. 2(a-b-c). The estimated thicknesses of the films are 294.44, 3101.1, and 4123.32 Å (thickness of substrate + layer), respectively. The fitted optical constants, i.e. the refractive indices and extinction coefficients, of films with different thicknesses of  $Sb_2S_3$  are presented in Figs. 3, 4 and 5, respectively.

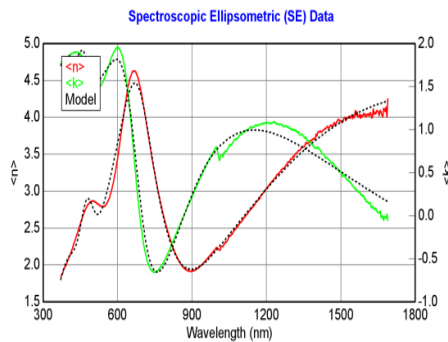


Fig. 3. Refractive index  $n$  and extinction coefficient  $k$  as a function of the wavelength of  $Sb_2S_3$  for the thickness = 300nm.

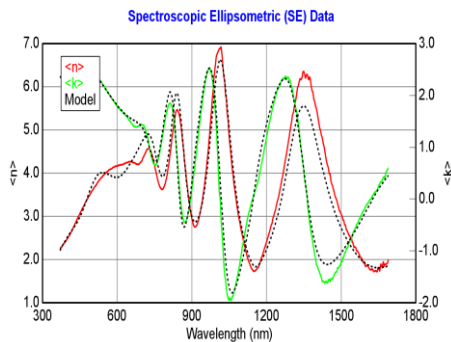


Fig. 4. Refractive index  $n$  and extinction coefficient  $k$  as a function of the wavelength of  $Sb_2S_3$  for the thickness = 500nm.

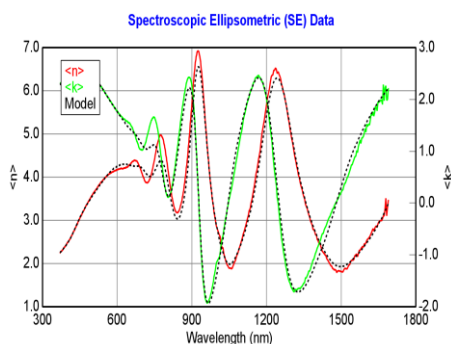


Fig. 5. Refractive index  $n$  and extinction coefficient  $k$  as a function of the wavelength of  $Sb_2S_3$  for the thickness = 800nm.

At each wavelength, the refractive index increases gradually with increasing the thickness of the  $Sb_2S_3$  film. The refractive index is closely related to the packing density of the films. Thus, the increase in the refractive index may be attributed to an increase in the packing density.

The absorption coefficient ( $\alpha h\nu$ ) of  $Sb_2S_3$  thin films can be calculated from the values of extinction coefficient  $k$  and  $\lambda$  using the known formula  $k = \alpha\lambda/4\pi$ . It is known that in the vicinity of the fundamental absorption edge, for allowed direct band-to-band transitions, the absorption coefficient is described by

$$\alpha(h\nu) = \frac{K(h\nu - E_g^{opt})^m}{h\nu}, \quad (3)$$

where  $K$  is a characteristic parameter (independent of photon energy) for the respective transitions,  $h\nu$  denotes the photon energy,  $E_g^{opt}$  is the optical energy gap and  $m$  is a number that characterizes the transition process.

Different authors [23–25] have suggested different values of  $m$  for different glasses:

$m = 2$  for most amorphous semiconductors (indirect transition) and  $m = 1/2$  for most crystalline semiconductors (direct transition). In a few reports, the band gap of  $Sb_2S_3$  is classified as direct [26, 27] and in others as indirect [28, 29]. Therefore, the allowed direct and indirect optical band gaps of  $Sb_2S_3$  films were evaluated from  $(\alpha h\nu)^2$  versus  $h\nu$  plots and  $(\alpha h\nu)^{1/2}$  versus  $h\nu$  plots, respectively.

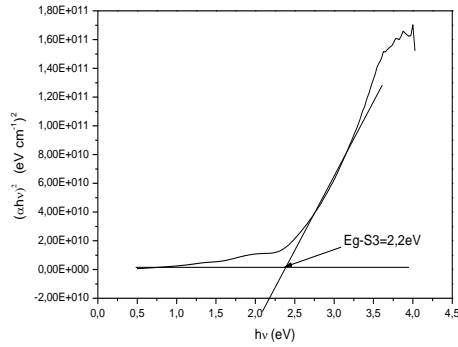


Fig. 6. Shows  $(\alpha hv)^2$  versus  $hv$  plots for films with different thicknesses of  $Sb_2S_3$ .

The  $(\alpha hv)^2$  versus  $hv$  plots of the  $Sb_2S_3$  films exhibited a straight line and the intercept of the energy axis at  $(\alpha hv)^2 = 0$  gave the direct energy band gap.

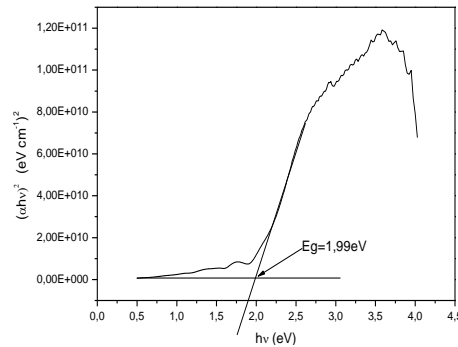


Fig. 7. Shows  $(\alpha hv)^2$  versus  $hv$  plots for films with different thicknesses of  $Sb_2S_3$ .

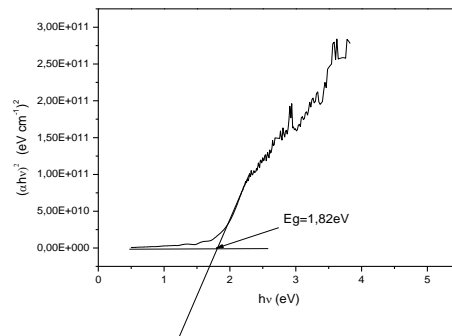


Fig. 8. Shows  $(\alpha hv)^2$  versus  $hv$  plots for films with different thicknesses of  $Sb_2S_3$ .

The variation of the direct band gap with thickness is shown in Fig. 9. Similarly, the indirect band gap of the films was evaluated from  $(\alpha hv)^{1/2}$  versus  $hv$  plots, as shown in Fig. 7, and its variation with thickness is also shown in Fig. 9. The values of  $E_{opt}$  for both direct and indirect transitions are found to increase with increasing the film thickness.

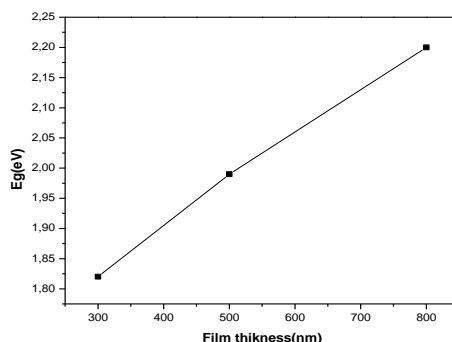


Fig. 9. Variation of band gap energy  $E_g$  vs film thickness of  $Sb_2S_3$  thin films.

The increase of  $E_{opt}$  for both direct and indirect transitions may be attributed to an increase in crystallite size.

#### 4. Conclusions

It is concluded from this study that  $Sb_2S_3$  thin film is a new material for solar cells that has potential for use as an absorber layer. The SE parameters ( $\Psi$  and  $\Delta$ ) for the  $Sb_2S_3$  films were measured in the wavelength range of 400–1800 nm and the optical constants of the  $Sb_2S_3$  films were determined by fitting the model function to the measured data using J A Woollam Corporation-developed WVASE32 program. The allowed direct and indirect optical band gaps of  $Sb_2S_3$  films were evaluated from  $(ah\nu)^2$  versus  $h\nu$  plots and  $(ah\nu)^{1/2}$  versus  $h\nu$  plots, respectively. Its optical properties were calculated by modeling the ellipsometry data to match with the reported absorber layers. The absorption coefficient is above is wavelength-dependent.

#### References

- [1] E. Perales, G. Lifante, F. Agullo-Rueda, C. de las Hares, J. Phys. D: Appl. Phys. **4**, 2440 (2007).
- [2] A. M. Salem, M. Soliman Selim, J. Phys. D: Appl. Phys. **34**, 12 (2001).
- [3] J. D. Desai, C. D. Lokhande, J. Non-Cyst. Solids **181**, 70 (1995).
- [4] K. C. Mandal, A. Mondal, J. Phys. Chem. Solids **51**, 1339 (1990).
- [5] O. Savadogo, K. C. Mandal, Solar Energy Mater. Solar Cells **2**, 117 (1992).
- [6] J. George, M. K. Radhakrishnan, Solid State Commun. **33**, 987 (1980).
- [7] I. Grozdanov, Semicond. Sci. Technol. **9**, 1234 (1994).
- [8] Z. S. El Mandouh, S. N. Salama, J. Mat. Sci. **25**, 1715, (1990).
- [9] Q. Lu, H. Zeng, Z. Wang, X. Cao, L. Zhang, Nanotechnology **17**, 2098, (2006).
- [10] O. Savadogo, K. C. Mandal, J. Electrochem. Soc. **139**, L16 (1992).
- [11] M. T. S. Nair, Y. Pena, J. Campos, V. M. Garcia, P. K. Nair, J. Electrochem. Soc. **145**, 2113 (1998).
- [12] R. S. Mane, B. R. Ankapol, C. D. Lokhande, Thin Solid Films **353**, 29 (1999).
- [13] R. S. Mane, C. D. Lokhande, Mater. Chem. Phys. **65**, 1 (2000).
- [14] B. R. Sankapal, R. S. Mane, C. D. Lokhande, J. Mater. Sci. Lett. **18**, 1453 (1999).
- [15] I. K. El Zawawi, A. Abdel-Moez, F. S. Terra, M. Mounir, Fizika **A7**(3), 97 (1998).
- [16] F. I Ezema, A. B. C. Ekwealor, R. U. Osuji, Turk. J. Phys. **30**, 157 (2006).
- [17] Fujiwara H 2007 Spectroscopic Ellipsometry: Principles and Applications (Chichester: Wiley).
- [18] J. W. Park, K. N. Choi, S. H. Baek, K. S. Chung, H. Lee, J. Korean Phys. Soc. **52**, 1868 (2008).
- [19] Y. Yamada, K. Tajima, M. Okada, S. Bao, M. Tazawa, K. Yoshimura, A. Roos, Phys. Status

- Solids C **5**, 1105 (2008).
- [20] J. H. Bhang, M. Lee, H. L. Park, I. W. Kim, J. H. Jeong, K. Kim, J. Appl. Phys. Lett. **79**, 1664 (2001).
- [21] E. A. Davis, N. F. Mott, Phil. Mag. **22**, 903 (1970).
- [22] E. R. Shaaban, Phil. Mag. **88**, 781(2008).
- [23] E. R. Shaaban, M. Abdel-Rahman, El. Sayed Yousef, M. T. Dessouky, Thin Solid Films **515**, 3810(2007).
- [24] M. Ichimura, K. Takeuchi, Y. Ono, E. Arai, Thin Solid Films **361–362**, 98(2000).
- [25] N. Koteswara Reddy, K. T. Ramakrishna Reddy, Thin Solid Films **325**, 4(1998).
- [26] Z. Zainal, M. Z. Hussein, A. Ghazali, Sol. Energy Mater. Sol. Cells **40**, 347(1996).
- [27] A. Ortiz, J. C. Alonso, M. Garcia, J. Toriz, Semicond. Sci. Technol. **11**, 243(1996).
- [28] E. A. El-Sayad, G. B Sakr, Cryst. Res. Technol. **40**, 1139 (2006).
- [29] H. S. Soliman, D. Abdel-Hady, E. Ibrahim, J. Phys.: Condens. Matter. **10**, 847 (1998).